Available online at www.sciencedirect.com

SciVerse ScienceDirect

Ceramics International 39 (2013) 2003–2011

CERAMICS INTERNATIONAL

www.elsevier.com/locate/ceramint

In vitro bioactivity and biocompatibility of a Co–Cr–Mo alloy after heat treatment in contact with different bioactive systems

R. Martínez[a], J.C. Escobedo[a], D.A. Cortés[a], G.G. Alves[b,c], A.B.R. Linhares[c], J.M. Granjeiro[b,c,d], M. Prado[e], J.C. Ortiz[a], J.M. Almanza[a], E.M. Múzquiz-Ramos[a,f,*]

[a]*CINVESTAV-Unidad Saltillo, Carretera Saltillo-Monterrey Km 13, Apartado Postal 663, C.P. 25000 Saltillo, Coahuila, México*
[b]*Department of Cell and Molecular Biology, Fluminense Federal University, Niteroi, Rio de Janeiro, Brazil*
[c]*Clinical Research Unit, Antonio Pedro Hospital, Fluminense Federal University, Niteroi, Rio de Janeiro, Brazil*
[d]*National Institute for Metrology, Quality and Technology, INMETRO, Duque de Caxias, Rio de Janeiro, Brazil*
[e]*Military Institute of Engineering (IME), Praça General Tibúrcio 80, CEP 22453-900, Urca, Rio de Janeiro, Brazil*
[f]*Facultad de Ciencias Químicas, Universidad Autónoma de Coahuila, Boulevard Venustiano Carranza y José Cárdenas, C.P. 25280, Saltillo, Coahuila, México*

Received 31 July 2012; accepted 17 August 2012
Available online 31 August 2012

Abstract

As-cast samples of a cobalt base alloy (ASTM F-75) were heat treated in contact with different bioactive materials: (a) powder mixtures of β-tricalcium phosphate (TCP)–bioactive glass (BG) in different proportions (TCP–BG: 60–40, 70–30 and 80–20 wt%) and (b) mineral and synthetic wollastonite. Samples were packed with each bioactive material and heat treated for 1 h at 1220 °C. To characterize the *in vitro* bioactivity, heat treated samples were immersed in a simulated body fluid. After immersion, a ceramic layer containing Ca and P was formed on all samples. The thicker and more homogeneous layers, identified as apatite, were formed more rapidly on the heat treated samples in contact with 80TCP–20BG and synthetic wollastonite. The more bioactive coatings were selected for MC3T3 cell adhesion, proliferation and differentiation assays. Cell proliferation and alkaline phosphatase activity were not affected by the different coatings. Additionally, samples packed with 80TCP–20BG presented a higher cell adhesion than those packed with synthetic wollastonite. On the samples previously packed with synthetic wollastonite, a denser homogeneous Ca- and P-rich layer was formed 21 days after cell seeding and incubation in differentiative conditions.

Keywords: Bioactivity; Cobalt base alloys; Cell culture; Bioactive ceramics

1. Introduction

The Co–Cr–Mo alloy (ASTM F-75) [1] is one of the most widely employed alloys in the manufacture of hip replacement prostheses due to its high corrosion resistance as well as its relatively simple and the low cost processing method. One of the main disadvantages of this alloy is that it presents very low levels of osseointegration and, therefore, it is classified as a bioinert material [2]. To overcome this disadvantage, bioactive ceramic coatings are widely used [3].

As stated in the literature [4], a bone-like apatite layer is formed on the surface of bioactive materials such as hydroxyapatite (HA), tricalcium phosphate (TCP), wollastonite, bioactive glasses and glass-ceramics when these materials are in contact with real or simulated body fluids [5–9]. In previous works, it has been demonstrated the feasibility of trapping bioactive materials on the ASTM F75 alloy during casting or the required heat treatment for this alloy [10]. The alloy was also described as presenting a high *in vitro* bioactivity after immersion on simulated body fluid (SBF) [11]. Also, it was demonstrated that the

*Corresponding author at: CINVESTAV IPN-Unidad Saltillo, Carretera Saltillo-Monterrey, Km 13, Apartado Postal 663, C.P. 25000 Saltillo, Coahuila, México. Tel.: +52 844 4389600 x 9683; fax: +52 844 4389610.
E-mail addresses: dora.cortes@cinvestav.edu.mx (D.A. Cortés), emuzquiz@uadec.edu.mx (E.M. Múzquiz-Ramos).

0272-8842/$ - see front matter © 2012 Elsevier Ltd and Techna Group S.r.l. All rights reserved.
http://dx.doi.org/10.1016/j.ceramint.2012.08.052

bioactivation of the cobalt base alloy resulted to be more appropriate during the required heat treatment at 1220 °C (with the objective of improving the ductility of the alloy), than when performed during casting [11].

However, other still unanswered questions remain to be issued in order to obtain better results with surface coating of the ASTM F-75 alloy for the development of medical devices. Among those, it is possible to include the following: (i) how the choice of coating materials (TCP, wollastonite, HA, bioactive glasses and so forth) influence the bioactivity of this alloy after treatment with body fluids? and (ii) would the surface bioactivity for those different coatings directly correlate to their biocompatibilities? In order to issue those questions, we have characterized the *in vitro* bioactivity of three different coatings for the Co–Cr–Mo alloy: powder mixtures of β-tricalcium phosphate–bioactive glass (TCP–BG) or either mineral (MW) or sol–gel synthesized (SW) powder wollastonite. The effect of the TCP to BG ratio on the *in vitro* bioactivity was evaluated using SBF. In addition, a comparison was performed between the use of (MW) and (SW) [12]. In order to assess the biocompatibility of the most bioactive materials identified, it was also evaluated the *in vitro* response of murine pre-osteoblasts, by measuring cellular adhesion, proliferation and differentiation in direct contact with the materials surfaces.

2. Materials and methods

2.1. Material preparation

A biocompatible cobalt base alloy (Biodur ASTM F75, Carpenter, USA) was used to obtain metallic discs of 1.27 cm in diameter and 0.5 cm in thickness. One of the flat surfaces of these discs was ground with SiC papers ranging from 80 to 2400 grit and polished using 30 μm and 10 μm diamond pastes. After polishing, the samples were gently washed for 5 min in ethanol using an ultrasonic bath.

The bioactive glass (BG) used in this study was prepared from a mixture of reagent grade chemicals of SiO_2, Na_2O, CaO and P_2O_5 (Sigma-Aldrich). The aim was to obtain a glass with a close composition to that of Bioglass® 45S5 [4]. The mixture was heated at 1360 °C and poured in an ice-cooled stainless steel plate. The glass was crushed in a laboratory planetary-type agate ball mill obtaining an average particle size of 36.75 μm.

The β-tricalcium phosphate (TCP) was obtained from a mixture of reagent grade chemicals of $CaCO_3$ and $(NH_4)_2HPO_4$ (Sigma-Aldrich). The mixture was heated (900 °C, 5 h), followed by sintering (1000 °C, 12 h). Once the product was cooled at room temperature, this was crushed in a laboratory planetary-type agate ball mill obtaining an average particle size of 30.41 μm.

The wollastonite was synthesized using the sol–gel method (under acid conditions) from the reagent grade chemicals of $Si(OCH_2CH_3)_4$ (tetraethyl orthosilicate, TEOS), HNO_3 (3%) and $Ca(NO_3)_24H_2O$ (Sigma-Aldrich). The TEOS was homogenized in deionized water (ratio H_2O/TEOS equal to 8) and then mixed with the appropriate amounts of nitric acid and tetra-hydrated calcium nitrate. After homogenization (room temperature, 5 h) and sol-aging (70 °C, 72 h), the obtained gel was dried (120 °C, 48 h) and heat treated (1300 °C, 3 h). The average size of the synthetic wollastonite was 11.0 μm. The mineral wollastonite was obtained commercially (Gosa, SA). The average particle size of the mineral wollastonite was 18.36 μm.

2.2. Packing of the metallic samples with bioactive powders

Two discs with 5 g of the selected bioactive material between them (sandwich-like) were placed into a metallic die. The mirror finished surface of each disc was selected for being in contact with the ceramic or powder bioactive mixtures. A uniaxial pressure of 65 MPa was applied for 45 s to the die using a hydraulic press (CAVER, 4350-L). After pressing the sandwiches, these were placed into alumina crucibles and covered with graphite in order to avoid alloy decarburation.

2.3. Heat treatment

The crucibles containing the sandwich samples were placed in an electric furnace (LINDBERG/BLUE, BF51433PC-1). The heat treatment was performed at 1220 °C for 1 h followed by quenching in water [13]. Finally, the specimens were washed with deionized water, dried in air at 130 °C for 2 h and stored in a desiccator before testing.

2.4. Immersion of heat-treated samples in simulated body fluid (SBF)

After heat treatment each metallic sample was immersed in 150 mL of SBF [14] at physiological conditions of pH and temperature for different periods of time. Then, the samples were gently washed with deionized water. Table 1 shows the description and identification of the samples obtained.

2.5. Bioactivity assessment

Both the surface and the cross-section of the metallic samples were analyzed by scanning electron microscopy (SEM, Philips, XL 30 ESEM). The acceleration voltage was 20 keV. The chemical composition of the ceramic material trapped on the samples was determined by energy dispersive spectroscopy (EDS, Software Genesis, EDAX). The Ca/P atomic ratio was calculated from the EDS analysis. The identification of the phases present in the raw materials, samples (ceramic or metallic) and on the ceramic coatings was performed by X-ray diffraction (XRD, Xpert Philips, PW3040) within a 2θ range from

Table 1
Experimental design of the *in vitro* bioactivation of the ASTM F75 alloy.

Sample ID	Bioactive packing material					Immersion periods in SBF		
	60% TCP–40% BG	70% TCP–30% BG	80% TCP–20% BG	100% WM	100% WS	7 days	14 days	21 days
60TCP–40BG	✓					✓	✓	✓
70TCP–30BG		✓				✓	✓	✓
80TCP–20BG			✓			✓	✓	✓
WM				✓		✓	✓	✓
WS					✓	✓	✓	✓

10° to 80° at a speed of 2°/min with a step of 0.02° using Cu Kα, 40 kV and 35 mA.

2.6. Biocompatibility evaluation

2.6.1. Cell culture

For the evaluation of the specific biocompatibility, as defined by Kirkpatrick and Mittermayer [15], of the diverse material surfaces from this study, only the materials which presented higher levels of *in vitro* bioactivity after immersion in SBF were selected: metallic discs packed with the mixture of 80 wt% β-tricalcium phospate–20 wt% bioactive glass and synthetic wollastonite. These samples were analyzed by cell proliferation, adhesion and differentiation assays.

MC3T3-E1 mouse preosteoblasts were cultured on Minimum Essential Medium (MEM) Alpha Medium (Gibco) at 37 °C with a 5% CO_2 atmosphere in a humidified incubator. The culture medium was supplemented with 10% fetal bovine serum (FBS) and replaced every 2 days. After sterilization of the metallic samples by long UV light exposition, they were placed on sterile 24-well culture plates and fixed with 500 μL agar–agar per well as a restrictive medium, leaving only the coated surface of the discs for cell adhesion/proliferation. MC3T3 cells were seeded onto the material surfaces at a density of 4.3×10^3 cells/cm^2 and incubated for different periods of time.

In order to observe the overall morphology of adhered cells, the samples were processed for scanning electron microscopy (SEM) by a 2 h fixation in 2.5% glutaraldehyde in 0.1 M Phosphate Buffered Solution (PBS, Sigma) at room temperature. After this, the samples were washed 3 times with PBS for 10 min each time and a post-fixation was then performed using 1% osmium tetraoxide with potassium ferrocyanide in 0.1 M PBS during 2 h. The samples were then gradually dehydrated on increasing concentrations of ethanol (from 30 to 100%). The dehydrated samples were critical point dried under the following conditions: CO_2, 31.1 °C and 1072 psi. Finally, the samples were coated with Au.

2.6.2. Cell adhesion and proliferation

The levels of cell adhesion were evaluated either 4 or 24 h after cell seeding by the Neutral Red (NR) assay [16]. Samples were incubated with culture medium containing excess Neutral Red vital dye for 3 h then washed, fixed and submitted to NR extraction on an ethanol/acetic acid solution. The Optical Density (O.D.) at 540 nm, which is proportional to the amount of living adhered cells, was measured on a microplate reader (Sinergy II, Biotek Instruments). Discs of uncoated ASTM F75 alloy and thermanox coverslips were employed as controls and the results are presented as a percentage of the thermanox control group. The same methodology described above allowed to infer possible differences on cell proliferation over diverse material surfaces after 3 or 7 days of cell seeding. Thermanox discs were used as the control group.

2.6.3. Cell differentiation

In order to study possible effects of the coatings over MC3T3 cells differentiation into a more mature osteoblastic stage, those cells were seeded over the different surfaces and incubated for 7, 14 or 21 days on Osteogenic Conditions (OC), induced by the supplementation of culture medium with 3 mM β-glicerolfphosphate and 50 μg ascorbic acid. The alkaline phosphatase (ALP) activity, a well-known marker of the early phases of osteoblast maturation/differentiation [17], was measured with a commercial kit (Falc-PP, Goldanalisa, Brazil), based on its capacity of hydrolyzing p-nitrophenyl phosphate (PNPP) in alkaline conditions, releasing p-nitrophenol (PNP) and inorganic phosphate into the culture medium. The kinetics for the release of PNP, measured colorimetrically, is directly proportional to the enzymatic activity of the alkaline phosphatase in each sample. Briefly, 50 μL of the PNPP solution was placed in a sterile 48-well culture plate and incubated at 37 °C for 5 min. After the pre-incubation, 10 μL of each sample was added. The Optical Density (O.D.) at 405 nm for each sample was measured with a Microplate Reader (Sinergy II, Biotek instruments) by 20 min at 37 °C, with 30 s intervals. The angular coefficient for each curve obtained by plotting time versus O.D. (at 405 nm) was obtained by a linear regression and converted to International Units (IU) by applying the milimolar extinction coefficient for the PNP product of 18.45 (at 405 nm). The activity was then normalized by the estimated cell density of each sample, through the division of the UIs by the O.D. (at 540 nm) from the Neutral Red test of their respective samples.

Table 2
Experimental design of the *in vitro* tests performed using MC3T3 cells.

Test	Replications	Time periods	Number of samples	Assay method
Adhesion 4 and 24 h	3	2	6	Alkaline phosphatase and SEM
Proliferation (1, 3, 5 and 7 days)	3	4	12	Alkaline phosphatase
Differentiation (14 and 28 days)	3	2	6	Alkaline phosphatase and SEM

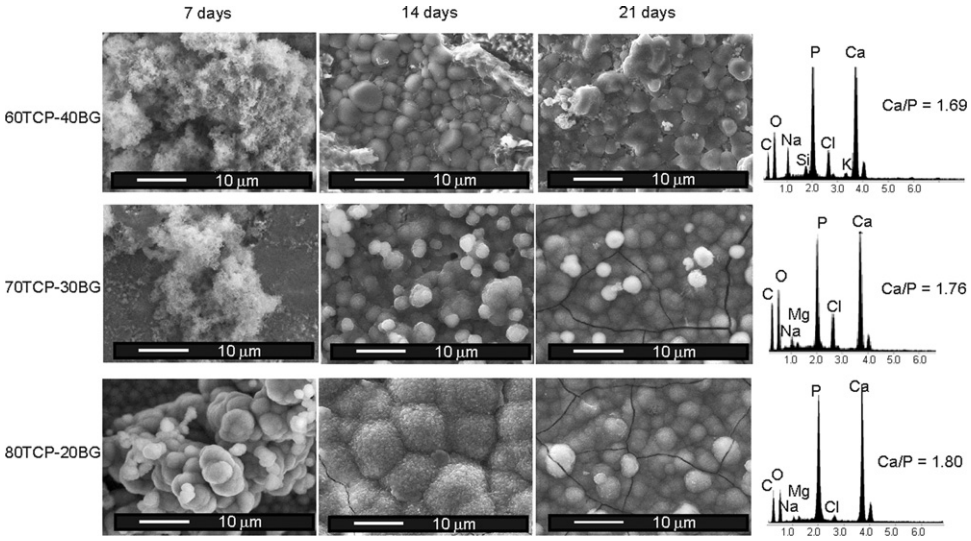

Fig. 1. SEM images of the metallic samples that were previously packed with the different TCP–BG mixtures after different immersion periods in SBF.

2.7. Statistical analysis

The results obtained from the biocompatibility assays (cell adhesion, proliferation and differentiation, $n=3$ each) were submitted to a Two-way Analysis of Variance (2-way ANOVA), with experimental time and material as factors (Table 2). The F statistics, at a significance level $\alpha=0.05$, indicated the factors and their interactions accountable for the statistically significant differences. A Bonferroni post-test was employed for identifying the statistically significant differences. All tests were performed with the help of the software GraphPad Prism 5.0.

3. Results and discussion

As we reported previously, after heat treatment, fine agglomerates were observed homogeneously distributed on the metallic surface, containing mainly Ca, P, O and Si. In the cases when the samples were packed using the mixture TCP–BG, Na was also detected [10,11].

Fig. 1 shows SEM images of the metallic samples that were previously packed with the different TCP–BG mixtures after different immersion periods in SBF. Agglomerates of a Ca- and P-rich compound were formed on all the samples after only 7 days of immersion in SBF. In all cases, a dense and homogeneous Ca- and P-rich layer was formed on samples after 14 days of immersion in SBF. After 21 days, this layer is considerably thick and its morphology closely resembles that observed on the existing bioactive systems [10]. The Ca/P atomic ratios (after 21 days) are within the range of the bone apatites, 1.2–1.7 [18]. As observed in the EDS spectrum of the sample identified as 80TCP–20BG, the intensity of the peaks corresponding to the substrate and those of the bioactive materials trapped during heat treatment is smaller than in the other cases. This indicates that this sample shows a higher bioactivity than that shown by the other compositions.

Fig. 2 shows SEM images of the metallic samples that were previously packed either in mineral or synthetic wollastonite after different immersion periods in SBF. A Ca- and P-rich layer was formed in all the cases and the behavior, morphology and Ca/P ratios are similar to those corresponding to the samples treated with the TCP80–BG20 system (Fig. 1). However, the sample treated with synthetic wollastonite demonstrated the highest *in vitro* bioactivity.

Fig. 3 shows the XRD patterns of the samples that were treated with the TCP–BG mixtures after different immersion periods in SBF. For the samples treated with either TCP60–BG40 or TCP70–BG30 mixtures after 7 or 14 days of immersion in SBF the phases detected by XRD are those corresponding to the alloy and Cr_2O_3. On the other hand, the ceramic compound formed after 21 days of immersion of this particular sample in SBF was identified

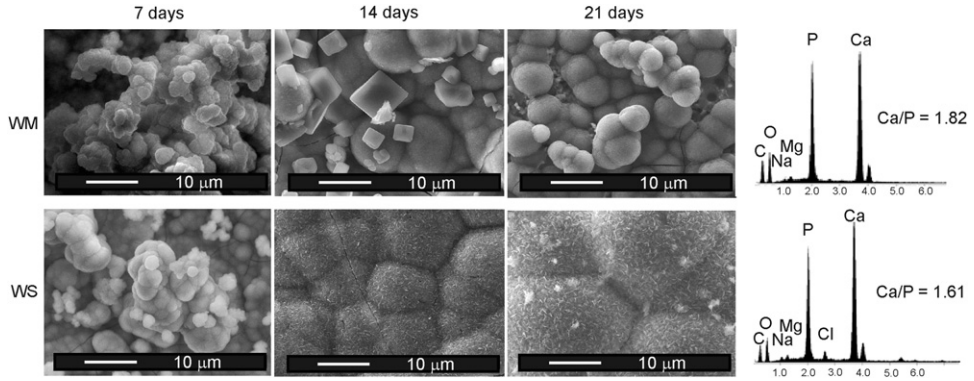

Fig. 2. SEM images of the metallic samples that were previously packed either with mineral or synthetic wollastonite after different immersion periods in SBF.

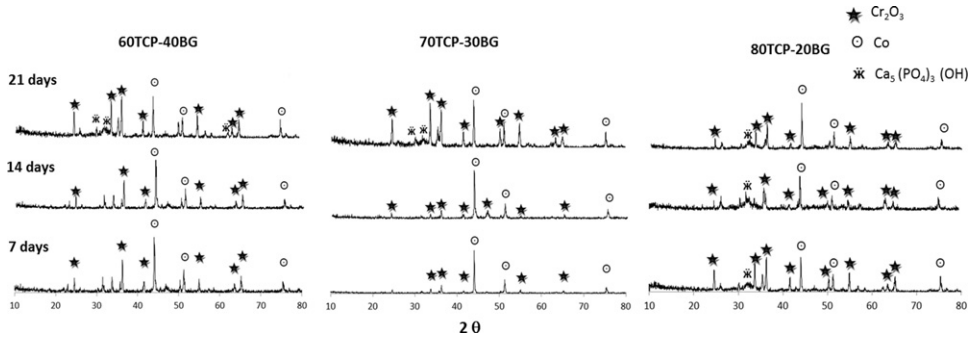

Fig. 3. XRD patterns of the metallic samples that were previously packed with the different TCP–BG mixtures after different immersion periods in SBF.

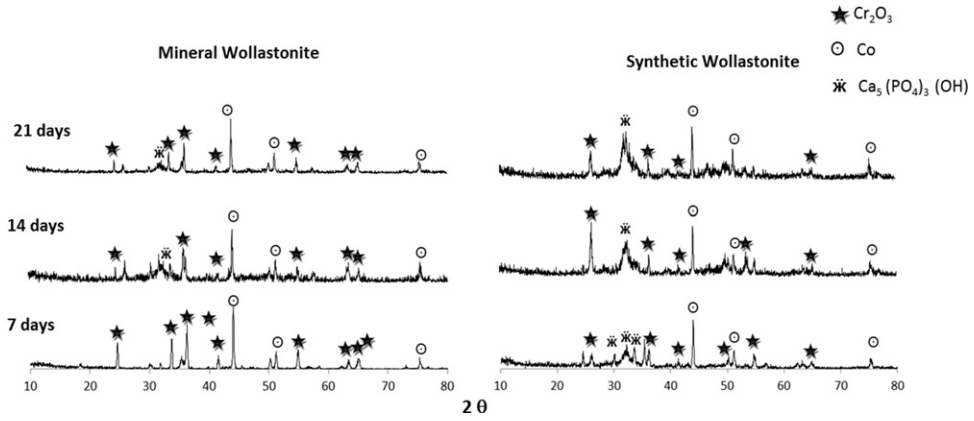

Fig. 4. XRD patterns of the metallic samples that were previously packed either with mineral (WM) or synthetic (WS) wollastonite after different immersion periods in SBF.

as hydroxyapatite (HA); peaks corresponding to the alloy and to the metallic oxide were also detected.

A completely different behavior was observed on the samples treated with the TCP80–BG20 mixture. After only 7 days of immersion in SBF, a peak at 31.7° 2θ corresponding to the (211) diffraction plane of apatite was detected in the corresponding pattern. These results are in agreement with those obtained by SEM analysis.

Fig. 4 shows the XRD patterns of the samples that were treated with either mineral (MW) or synthetic (SW) wollastonite after different immersion periods in SBF. The peak corresponding to apatite was identified only after 7 days of immersion in SBF of the sample treated with SW. However, on the sample treated with MW the apatite peak was detected only after 21 days of immersion in SBF.

Fig. 5 presents SEM images of the cross-section of the samples that were previously treated with TCP80–BG20 (Fig. 5a) or WS (Fig. 5b) after 21 days of immersion in SBF. A thicker apatite layer was formed on the sample

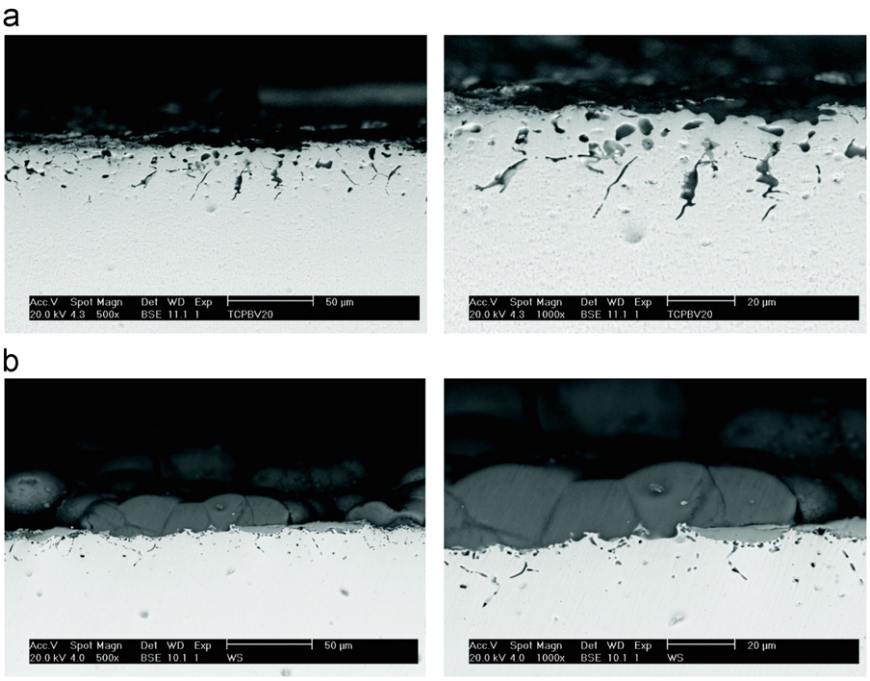

Fig. 5. Cross-section SEM images of the metallic samples treated with (a) 80TCP–20BG and (b) WS after 21 days of immersion in SBF.

treated with SW. In all the cases, three phases can be observed, the light gray-colored phase corresponds to the alloy, the medium gray phase corresponds to the metallic oxide formed during the heat treatment and the dark gray layer corresponds to apatite.

Based on the SEM, EDS and XRD results presented above, it was possible to select the most bioactive materials, namely the ASTM F75 discs treated with TCP80–BG20 or SW, for the *in vitro* biocompatibility evaluation. With this objective, three important parameters were selected for evaluation, namely (i) cell attachment, (ii) cell proliferation and (iii) osteoblast maturation/differentiation, as these are important factors studied on the interactions of biocompatibility of ceramic coatings on metals and alloys [19–22]. We also have chosen the MC3T3-E1 lineage, since these murine pre-osteoblasts are very representative of the mammal bone cells usually in contact with restorative devices.

Fig. 6A shows the relative levels of MC3T3 cell adhesion in direct contact with the samples, as compared to thermanox coverslips (control), as measured colorimetrically. As observed, the metallic samples that were treated with the TCP80–BG20 mixture demonstrated a higher cell attachment by 4 h than both the untreated alloy samples and those treated with SW ($p < 0.05$), attaining levels which are similar to the control. However, 24 h after seeding, the cell adhesion pattern changes significantly, since the cell density on the uncoated alloy reaches higher levels than both coated groups. These results may imply either a very transient attachment over TCP80–BG20 surfaces, or an initial proliferative rate, which is lower than that of the control and the uncoated alloy groups. At any rate, while comparing the two-coated groups, it is still possible to observe almost doubled levels of adhered cell at 24 h with TCP80–BG20, as compared to SW.

Fig. 7 presents SEM images showing the morphology of the MC3T3 cells during the attachment and adhesion times. MC3T3 cells seeded over uncoated ASTM-F75 (control) are well adhered and present a viable morphology already at 4 h after seeding (Fig. 7A). A more effective spreading and the formation of multiple cell layers could be observed at 24 h (Fig. 7B), reinforcing the good interaction with such surface.

An initial cell attachment was also observed with TCP80–BG20 surfaces (Fig. 7C), even though the cell morphology was less turgid, as compared to control. An apparent decrease on adhered cell density could be observed 24 h after seeding (Fig. 7D), possibly due to the irregularity on the pore size of the composite, or the migration of cell to the interior of the porous coat developed during heat treatment. The SW samples presented an apparent lower amount of cells attached by 4 h after seeding, even though with a very healthy cell morphology, presenting long cytoplasmic prolongations with several possible points of focal adhesion (Fig. 7E). By 24 h, adhered cell levels over SW (as qualitatively observed) seemed to strongly decrease (Fig. 7F).

As it was not expected, levels of viable cells over the different material surfaces were again followed colorimetrically for up to 1 week (Fig. 6B), it was possible to observe an increasing proliferative rate with SW and, at the same time, a slow down on the proliferation of cells over the uncoated alloy. As a result, both coated and uncoated samples presented no significant differences on attached cell levels by day 7, while all groups remained significantly lower than control (thermanox coverslips).

Finally, the levels of cell differentiation over the studied surfaces were inferred by the alkaline phosphatase activity (ALP) of the MC3T3 cells. Previous works from literature describe a peak of ALP activity usually for 2 weeks, with confluent MC3T3-E1 cells seeded over polystirene, and in the absence of dexamethasone [17]. However, the results from Fig. 8 show that, in this work, all groups presented maximum ALP activity by day 7, with a significant reduction ($p < 0.05$) on longer experimental times (14 and 21 days). Also, on all experimental times, the levels of ALP were significantly lower for the control thermanox group, regardless of considering total activity (data not shown) or normalization by cell density (Fig. 8). This pattern may be related to the higher proliferative state of cells over this surface, which is incompatible with high differentiation levels, which usually is the most notable after growth arrest [23]. Comparing the coated and uncoated alloy groups, only by day 7 there was a significant difference between the uncoated and the SW group, which disappeared by day 14. We could speculate, on the lights of the proliferation/differentiation dichotomy, that this difference among uncoated and SW coated alloys may be related to the observed proliferation rates during the first week after seeding. In a general manner, however, the kind of coating employed did not seem to affect the overall biological response of MC3T3 cells. When observed by SEM, the

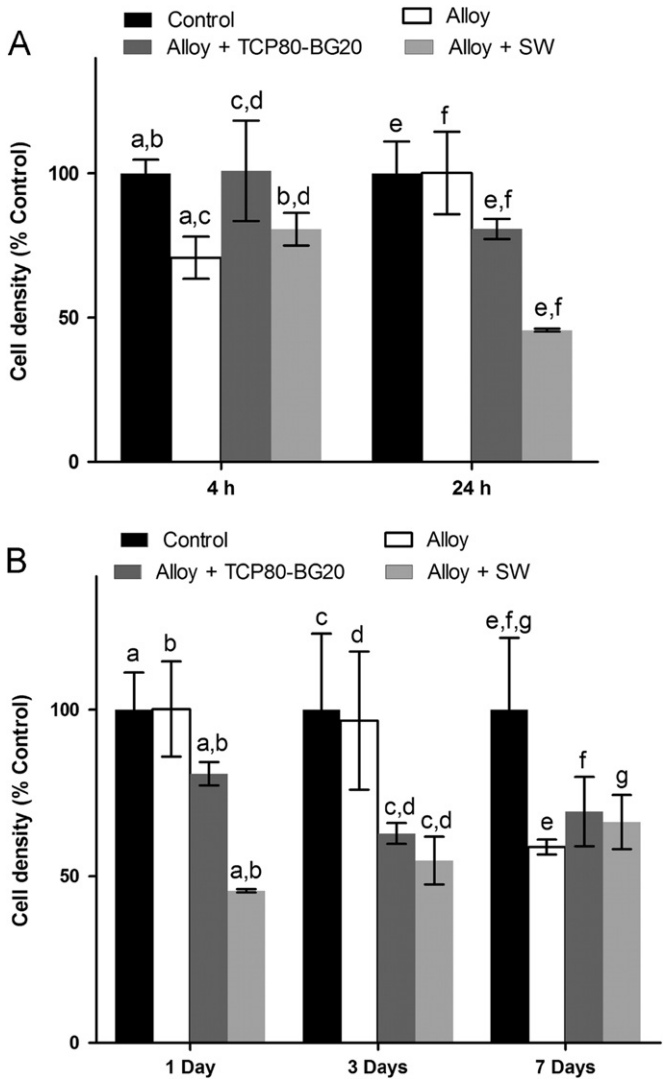

Fig. 6. MC3T3 cell response to the adhesion assay on samples after (A) 4 and 24 h and (B) 1, 3 and 7 days of culturing.

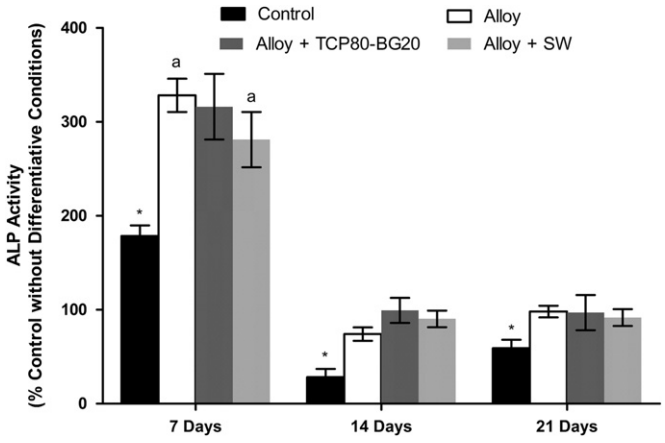

Fig. 8. MC3T3 cell response to the differentiation assay on the samples after 7, 14 and 21 days.

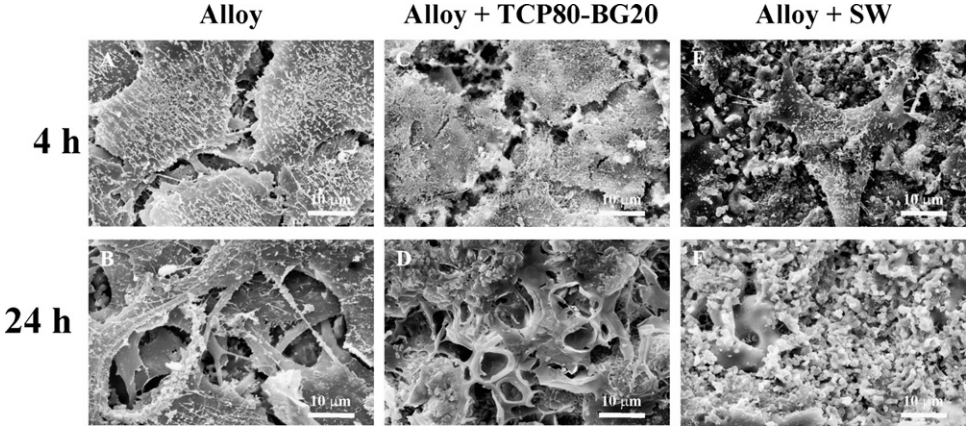

Fig. 7. SEM images of the morphology of the MC3T3 cells during the attachment and adhesion times.

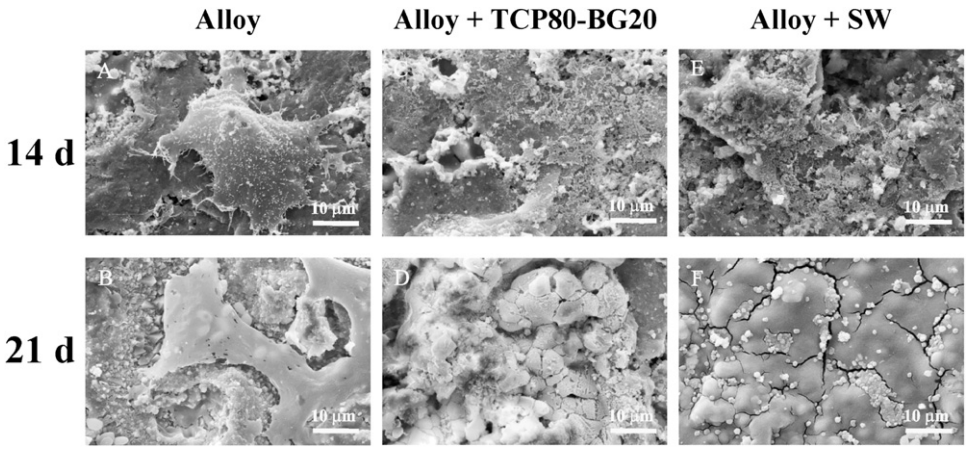

Fig. 9. SEM images of the morphology of the MC3T3 cells during the differentiation times.

interaction of these cells with the control alloy by day 14 is characterized by a marked spreading in multiple cell layers—a pre-requisite to the mineralization process on osteoblasts [24] (Fig. 9A). The strong presence of granules on the cell surface observed by 21 day (Fig. 9B) may be representative of such process. The presence of the TCP80–BG20 coating presented similarly innumerous granules over the entire material surface, including the cell layer, as early as 14 days after cell seeding, and forming an evident ceramic layer by 21 day (Fig. 9C and D). According to the EDS spectra analysis, the main elements detected were Si and O (data not shown). As reported previously [3], during the mechanism for apatite formation on bioactive glasses in SBF a SiO_2 gel is usually formed on the surface. It is possible that the compound formed on the materials treated with TCP80–BG20 in this work, corresponds to a SiO_2 gel. In the WS coated group, mineralization granules were also identified on cell surface after 14 days (Fig. 9E). After 21 days, a dense and homogeneous layer, Ca- and P-rich (as identified by EDS analysis), even thicker than that observed with TCP80–BG20, has completely covered the metallic sample and the cell layer (Fig. 9E). We may consider the possibility that this layer could be a result of the increased osteoblast mineralization on those samples, even though this supposition is not corroborated by the ALP assay, in which there was no indication of effects on osteoblast maturation between samples. On the other hand, it is also possible that this mineral layer is another effect of the strong bioactivity of SW coatings in the presence of culture media, as shown in this work. At any rate, the Ca, P mineralization process was stronger on SW, as compared to both TCP80–BG20 and uncoated alloy.

4. Conclusions

These results demonstrate the feasibility to promote a high *in vitro* bioactivity on the ASTM F-75 alloy using different bioactive materials during heat treatment, on a material-dependent manner. A higher bioactivity was observed when the samples were heat treated in contact with a mixture of TCP/BG on a proportion of 80:20, as well as with synthetic wollastonite. While TCP80–BG20 coatings may improve cell adhesion, a stronger Ca-, P-mineralization is promoted by SW coatings. Further studies are required to determine if these differences are sufficient to impact the outcome of clinical applications with such coated materials.

References

[1] ASTM Standard F75-07 Standard Specification for Cobalt-28 Chromium-6 Molybdenum Alloy Castings and Casting Alloy for Surgical Implants, ASTM F-75, ASTM International, 2001.
[2] M. Gomez, H. Mancha, A. Salinas, J.L. Rodriguez, J. Escobedo, M. Castro, Relationship between microstructure and ductility of investment cast ASTM F-75 implant alloy, Journal of Biomedical Materials Research 34 (1997) 157–163.
[3] T. Kokubo, H.M. Kim, M. Kawashita, Novel bioactive materials with different mechanical properties, Biomaterials 24 (2003) 2161–2175.
[4] L. Hench, O. Andersson, Bioactive glasses, in: J. Hench, T. Wilson (Eds.), An Introduction to Bioceramics, 1st ed., World Scientific, Florida, 1993, pp. 41–62.
[5] D.A. Cortes, A. Medina, J.C. Escobedo, S. Escobedo, M.A. Lopez, Effect of wollastonite ceramics and bioactive glass on the formation of a bonelike apatite layer on a cobalt base alloy, Journal of Biomedical Materials Research Part A 70 (2004) 341–346.
[6] P.N. De Aza, F. Guitian, F. De Aza, Bioactivity of wollastonite ceramics: in vitro evaluation, Scripta Metallurgica et Materialia 31 (1994) 1001–1005.
[7] X. Liu, C. Ding, Morphology of apatite formed on surface of wollastonite coating soaked in simulated body fluid, Materials Letters 57 (2002) 652–655.
[8] X. Liu, C. Ding, Reactivity of plasma-sprayed wollastonite coating in simulated body fluid, Journal of Biomedical Materials Research 59 (2002) 259–264.
[9] X. Liu, C. Ding, P.K. Chu, Mechanism of apatite formation on wollastonite coatings in simulated body fluids, Biomaterials 25 (2004) 1755–1761.
[10] J.M. Almanza, J.C. Escobedo, J.C. Ortiz, D.A. Cortés, Bioactivation of a cobalt alloy by coating with wollastonite during investment casting, Journal of Biomedical Materials Research A 78 (2006) 34–41.
[11] J.C. Ortiz, D.A. Cortes, J.C. Escobedo, J.M. Almanza, C.R. Muñiz, J.S. Luna, Bioactive coating on a cobalt base alloy by heat treatment, Materials Letters 65 (2011) 329–332.

[12] M.I. Alemany, P. Velasquez, M.A. De la Casa-Lillo, P.N. De Aza, Effect of material's processing methods on the 'in vitro' bioactivity of wollastonite glass-ceramic materials, Journal of Non-Crystalline Solids 351 (2005) 1716–1726.
[13] A. Salinas, M. Soria, H. López, Processing and Fabrication of Advanced Materials, The Minerals, Metals and Materials Society, 1996 vol. V.
[14] T. Kokubo, H. Takadama, How useful is SBF in predicting in vivo bone bioactivity?, Biomaterials 27 (2006) 2907–2915
[15] C.J. Kirkpatrick, C. Mittermayer, Theoretical and practical aspects of testing potential biomaterials in vitro, Journal of Materials Science—Materials in Medicine 1 (1990) 9–13.
[16] F.C. Kull, P. Cuatrecasas, Estimation of cell number by neutral red content—applications for proliferative and survival assays, Applied Biochemistry and Biotechnology 8 (1983) 97–103.
[17] C.D. Hoemann, H. El-Gabalawy, M.D. McKee, In vitro osteogenesis assays: influence of the primary cell source on alkaline phosphatase activity and mineralization, Pathologie-Biologie (Paris) 57 (2009) 318–323.
[18] T. Kokubo, H.M. Kim, M. Kawashita, Novel bioactive materials with different mechanical properties, Biomaterials 24 (2003) 2161–2175.
[19] L. Meseguer-Olmo, J. Muñoz-Ruiz, A. Bernabeu-Esclapez, M. Clavel-Sainz Nolla, D. Arcos-Pérez, M. Vallet-Regí, *In vitro* growth kinematics of human osteoblasts on porous hydroxyapatite ceramics, Revista de Ortopedia y Traumatología 50 (2006) 224–232.
[20] T.J. Webster, J.U. Ejiofor, Increased osteoblast adhesion on nanophase metals: Ti, Ti6Al4V, and CoCrMo, Biomaterials 25 (2004) 4731–4739.
[21] E. Zhang, C. Zou, G. Yu, Surface microstructure and cell biocompatibility of silicon-substituted hydroxyapatite coating on titanium substrate prepared by a biomimetic process, Materials Science and Engineering: C 29 (2009) 298–305.
[22] O. Zinger, K. Anselme, A. Denzer, P. Habersetzer, M. Wieland, J. Jeanfils, Time-dependent morphology and adhesion of osteoblastic cells on titanium model surfaces featuring scale-resolved topography, Biomaterials 25 (2004) 2695–2711.
[23] L.D. Quarles, D.A. Yohay, L.W. Lever, R. Caton, R.J. Wenstrup, Distinct proliferative and differentiated stages of murine MC3T3-E1 cells in culture: an in vitro model of osteoblast development, Journal of Bone and Mineral Research 7 (1992) 683–692.
[24] I. Gerber, I. ap Gwynn, Influence of cell isolation, cell culture density, and cell nutrition on differentiation of rat calvarial osteoblast-like cells in vitro, European Cells and Materials 2 (2001) 10–20.